UNILATERAL HIP JOINT SEGMENTATION WITH SHAPE PRIORS LEARNED FROM MISSING DATA

Shekhar Chandra[⋆] *Ying Xia*[⋆] *Craig Engstrom*[†] *Raphael Schwarz*[*] *Lars Lauer*[*] *Stuart Crozier*[†] *Olivier Salvado*[⋆] *Jurgen Fripp*[⋆]

[⋆] Australian e-Health Research Centre, CSIRO, Australia

[†] School of Human Movement Studies, The University of Queensland, Australia

[*] Siemens Healthcare, Germany

ABSTRACT

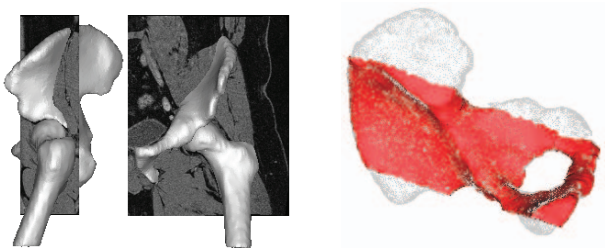
The accurate segmentation of the bone from Magnetic Resonance (MR) images of the hip is important for clinical studies and drug trials into conditions like Osteoarthritis. This paper presents an automatic segmentation scheme that utilises a deformable model robust to different field of views by training shape priors from partial and full bone surfaces. The deformable model with these priors were used to segment the hip joint within 16 unilateral 3T MR images having different field of views, so that parts of the model outside the image could be ignored fully without affecting the accuracy of the segmentation within the image. Mean and median Dice's Similarity Coefficients of 0.91 & 0.92 for the femur and 0.86 & 0.88 for one half of the pelvis were obtained using a leave-one-out approach.

Index Terms— Shape Model, Segmentation, Hip, Missing Data, Magnetic Resonance.

1. INTRODUCTION

Osteoarthritis (OA) is primarily a disease of the articular cartilage, which can cause pain, stiffness and decreased motion of large weight-bearing joints, such as the hip and knee [1]. It is characterized by changes in the structure and degeneration of the cartilage tissue. Early detection of OA may allow therapeutic treatments before permanent damage has developed and surgeries like arthroplasty are required.

Magnetic Resonance (MR) imaging has been shown to be an ideal imaging modality for OA assessment in the knee by providing direct and non-invasive visualization of joint structure with no ionizing radiation. It also provides multi-planar capability and high contrast between cartilage and other surrounding tissues [2]. However, in other joints including the hip, less studies have been performed to evaluate cartilage changes using MRI [3], although in recent years more are occurring [4]. One of the main reasons for this is the difficulty in handling different field of views (FOVs) of the images acquired. A small FOV is acquired because of the size of the hip joint and the relatively thin cartilage when compared to that of the knee. Figure 1(a) shows an example of an MR image with a small FOV.



(a) (b)

Fig. 1. (a) shows how the mean surface of the shape prior has a different FOV than a unilateral MR image. (b) shows how the missing points of a partial surface, with respect to the mean shape of the prior, can be recovered using the RPCA of Skočaj *et al.* [5].

The accurate localisation of the bone is a key initial step to segment the cartilage tissue of the joint. There have been several previous automated segmentation methods presented for the hip bone, such as demon-based registration to the anatomical atlas [6], or physically-based deformable models with shape priors [7]. However, those methods are not robust when the hip bone form deviates strongly, and has different FOVs, from the training data (see figure 1(a)). Different FOVs result naturally when imaging the hip joint with sufficient resolution for resolving both acetabular and femoral cartilages. Due to these issues, most clinical studies still utilise semi-automated methods [8]. Recently, Xia *et al.* [9] introduced a fully automatic approach to segment the bones of the hip using an deformable model approach. This scheme utilised an affine initialisation to deform a bone surface within the image and shape priors applied to all of the surface to keep it anatomically valid. The method was made more robust by disabling points outside the image during the deformations. However, they applied shape priors

to the entire surface, which introduced errors into the segmentation results.

Previous cartilage or acetabulum studies have been performed manually or semi-automatic segmentations [3]. Watanabe *et al.* [10] recently reported single-slice hip cartilage T2 measurements and its topographic variation on healthy volunteers. In some cases the femoral and acetabular cartilages are considered jointly, although using an upsampling of the hip MR data by a factor of 10, accurate and repeatable separable segmentations can be performed [11]. Both these methods are time-consuming and require a skilled and experienced operator.

In this paper, we present a fully automated segmentation scheme based on a robust deformable model that can handle different FOVs. This scheme utilises a robust shape model that can be trained from multi-modal surface data and one that can be applied to partial surfaces, such as parts of a surface inside an image (see figure 1). These shape priors are trained from Computed Tomography (CT) and MR surface data using the Robust Principal Component Analysis (RPCA) of Skočaj *et al.* [5]. The multi-modal surfaces possess missing data with respect to their mean shape, and the RPCA can be used to recover the missing data to allow the application of shape priors accurately to the current FOV (see figure 1). This allows the mean shape to be initialised and placed into a unilateral MR image having an arbitrary FOV and deformed to the bone boundaries using image gradient information, while applying shape priors only to the parts of the surface present within the image.

The following section describes the segmentation pipeline and section 3 presents the results of the method when applied to a number of unilateral MR images.

2. METHOD

A total of 16 unilateral MR images were created from 16 bilateral MR images acquired on a 3T Siemens Trio Scanner at the University of Queensland. A simple automatic cropping was performed on the bilateral images by bisecting the x-axis to produce two halves (left and right side) of the hip. Four parts of the hip bone (left/right femur, left/right pelvis) were manually segmented in each bilateral MR image by Y.X using ITK-SNAP [12] with expert guidance from C.E. The same cropping was applied to the labels of the bilateral images to produce corresponding unilateral labels for each case. To train the shape priors, the CT atlas pelvis and femoral surfaces were propagated to the 28 CT cases from Calvary Mater Newcastle Hospital, as well as the 16 contoured MR cases. The MR cases were then automatically segmented using a deformable model with a leave-one-out approach.

The deformable model in this work consists of a surface $\boldsymbol{S}$, a surface regularisation method and bone shape priors, which are trained from manual contours. The surface is composed of vertices $\boldsymbol{v}_i$, where $0 \leqslant i < N$ and N is the number of points. The remaining parts of this section is devoted to the description of the robust shape constraints.

2.1. Model Building

Shape priors are usually trained from a series of surfaces with point correspondence [13]. The shape model is obtained by aligning the surfaces via Generalised Procrustes Alignment (GPA) and applying Principal Component Analysis (PCA) to the points to get the shape priors. However, the PCA requires complete surfaces and only allows the application of shape priors to the entire surface. In this work, the shape priors are required to handle partial surfaces, in particular, those parts of a surface inside an image.

The RPCA, via the iterative reconstruction algorithm of Skočaj *et al.* [5], allows learning from missing data. The known data from partial or full surfaces is reordered to preserve point correspondence and the unknown data marked as missing. In this work, the shape priors were reordered for the RPCA as follows:

1. The CT atlas surface is propagated and matched to the manual contours of the training set, so that the training surfaces are deformed versions of the same mesh, while representing the manual contours as closely as possible. Thus, all the training surfaces have correspondence and one may easily reorder points to preserve correspondence and mark missing points.

2. Align points using GPA.

3. Clip surfaces to remove points outside the image.

4. Create the covariance matrix $\boldsymbol{C}$ from the full or partial surfaces by reordering the known points with respect to the correspondence.

The RPCA algorithm, given the weight matrix $\boldsymbol{W}$ having the weights of the known and unknown points to one and zero respectively, is as follows:

1. The weighted mean surface $\boldsymbol{\mu}$ is removed from $\boldsymbol{C}$.

2. The RPCA is initialised by applying the standard PCA on $\boldsymbol{C}$ to produce an eigen-decomposition, with eigenvectors $\boldsymbol{U} = [\boldsymbol{u}_1, \ldots, \boldsymbol{u}_N] = \boldsymbol{u}_i$ and eigenvalues λ_i, so that variation of the known data is modelled.

3. The result is a set of modes that model how each vertex varies from the mean vertex given the training surfaces, so that one can project a shape $\boldsymbol{S} =$

$[\boldsymbol{v}_1, \ldots, \boldsymbol{v}_N] = \boldsymbol{v}_i$ as

$$\boldsymbol{b}_i = \bar{\boldsymbol{U}}^T (\boldsymbol{v}_i - \boldsymbol{\mu}), \quad (1)$$

into the variation (PCA) model to acquire the variation coefficients $\boldsymbol{b}_i$, where $\bar{\boldsymbol{U}}$ is the weighted version of, i.e. the Hadamard product with, $\boldsymbol{U}$.

4. The training surfaces, together with the missing points in $\boldsymbol{C}$, are reconstructed from these coefficients and the un-weighted eigenvectors as

$$\hat{\boldsymbol{v}}_i = \sum_j^s b_{ji} u_{ji} + \boldsymbol{\mu}, \quad (2)$$

where s is the number of training surfaces.

5. The missing points in $\boldsymbol{C}$ are replaced with the reconstructed values and the PCA is applied again. The process is repeated from step 3 until convergence.

The RPCA also allows applying the trained constraints to partial surfaces. Points which are considered to be outliers or erroneous can be marked as missing and the current training data used to replace these points with reconstructed values iteratively. In this way, the known points may be reconstructed accurately within the trained constraints of the shape priors, while the missing parts are replaced with approximate values that reflect the reconstruction of the known points. The result is shape constraints tailored to the points inside the image, allowing more accurate reconstructions. After the constraints are applied, the deformation, regularisation and shape prior processes are repeated until convergence of the surface to the bone boundaries.

2.2. Segmentation Scheme

The deformable model was applied as follows:

1. The surface was initialised to a new MR by an affine registration of a bilateral CT atlas divided into left and right parts. The CT atlas was created from a set of 28 scans of the pelvis from a Prostate Cancer study at Calvary Mater Newcastle Hospital that were semi-automatically labelled using an atlas based registration approach. The mean surface of the labels corresponding to the CT atlas, extracted using the marching cubes algorithm, was propagated to the new case using the affine transform.

2. The surface was deformed to the local boundaries in proximity to the surface within the image. The displacements of each vertex were determined from the mean gradient within one dimensional (1D) profiles extracted along the vertex normals of the surface. These deformations are computed independently of neighbouring vertex displacements.

3. The irregular shape caused by the individual vertex deformations was regularised by using the weighted sums of the neighbouring vertices to re-adjust the position of each vertex.

4. The parts of the surface outside the image were clipped.

5. The robust shape model was used to apply shape constraints to the remaining parts of the surface to keep its shape anatomically valid.

6. Once the above steps converge, the Bone Cartilage Interface (BCI) was extracted using the resultant bone segmentations.

3. RESULTS

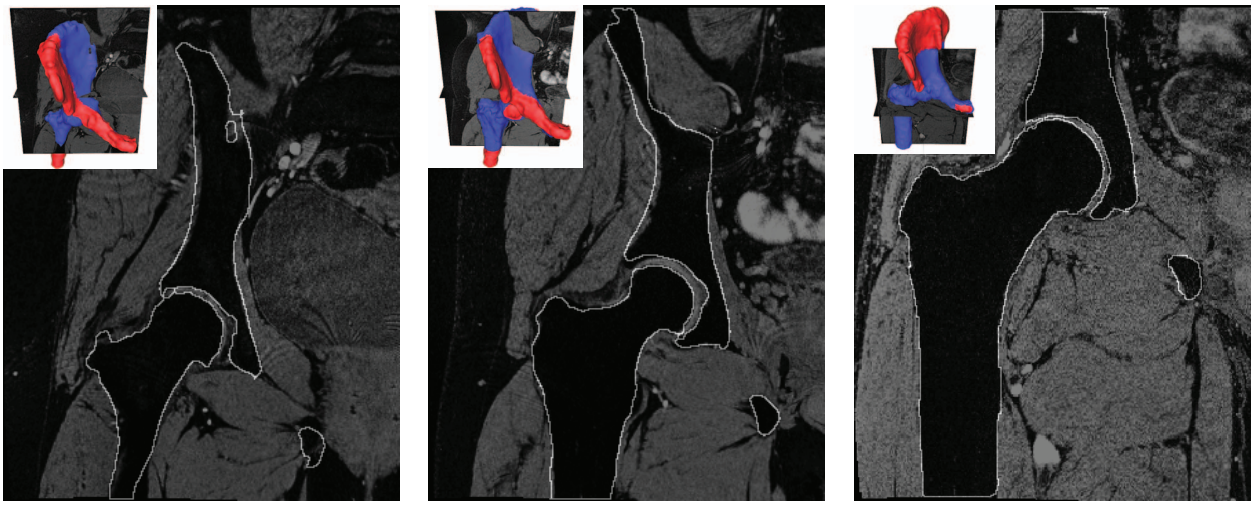
Figure 1(b) shows the reconstruction of a partial surface (with points outside an MR image removed) by the trained robust shape priors. The qualitative results for three cases can be seen in figure 2 shown as overlays on the MR images. Table 1 summarises the results obtained for the robust deformable model approach for the 16 MR images with the mean Dice's Similarity Coefficient (DSC) shown in bold. Figure 3 shows the preliminary BCI extracted from the bone segmentation results of table 1. Further work needs to be done in utilising a more robust GPA algorithm to also handle different FOVs, as well as adding cartilage segmentation to the pipeline after improving the bone segmentations and BCI quailty.

Table 1. Results for the unilateral MR images.

Bone	**Mean DSC**	Median DSC	Min DSC	Max DSC	Sens.	Iterations	Profile Len./Spac.
Acetabulum	**0.86**	0.88	0.73	0.91	0.89	20	16/0.35mm
Femur	**0.91**	0.92	0.78	0.95	0.89	10	32/0.35mm

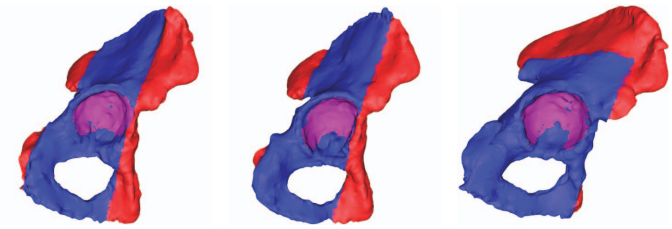
4. CONCLUSION

This paper presented a novel and robust deformable model approach to automatically segment unilateral MR images that could handle different FOVs. The iterative reconstruction algorithm of the RPCA could recover the missing parts of surfaces (such as those outside unilateral images), allowing shape priors to be applied to accurately to known parts of a surface. This resulted in segmentations of sufficient quality, having a mean DSC of 0.91 and 0.86 for the femur and pelvis respectively (see figure 2 and table 1), that can be used for cartilage analysis in the future.



(a) (b) (c)

Fig. 2. (a)-(c) shows the segmentation results, overlaid as contours on the MR images, for cases 9, 11 and 16 respectively. Inset shows a 3D view of the results, where blue regions indicate parts of the surface within the image.



(a) (b) (c)

Fig. 3. BCI results (purple) for cases 9, 11 and 16.

5. REFERENCES

[1] R. D. Altman, D. A. Bloch, M. Dougados, M. Hochberg, S. Lohmander, K. Pavelka, T. Spector, and E. Vignon, "Measurement of structural progression in osteoarthritis of the hip: the barcelona consensus group," *Osteoarthritis and Cartilage*, vol. 12, no. 7, pp. 515– 524, 2004.

[2] D Burstein, A Bashir, and M L Gray, "MRI techniques in early stages of cartilage disease," *Investigative Radiology*, vol. 35, no. 10, pp. 622–638, Oct. 2000.

[3] G. Zhai, F. Cicuttini, V. Srikanth, H. Cooley, C. Ding, and G. Jones, "Factors associated with hip cartilage volume measured by magnetic resonance imaging: The Tasmanian Older Adult Cohort Study," *Arthritis & Rheumatism*, vol. 52, no. 4, pp. 1069–1076, Apr. 2005.

[4] J. Carballido-Gamio, T. M. Link, X. Li, E. T. Han, R. Krug, M. D. Ries, and S. Majumdar, "Feasibility and reproducibility of relaxometry, morphometric, and geometrical measurements of the hip joint with magnetic resonance imaging at 3T," *Journal of Magnetic Resonance Imaging: JMRI*, vol. 28, no. 1, pp. 227–235, July 2008.

[5] Danijel Skočaj, Aleš Leonardis, and Horst Bischof, "Weighted and robust learning of subspace representations," *Pattern Recognition*, vol. 40, no. 5, pp. 1556–1569, May 2007.

[6] J Ehrhardt, H Handels, T Malina, B Strathmann, W Plötz, and S J Pöppl, "Atlas-based segmentation of bone structures to support the virtual planning of hip operations," *International Journal of Medical Informatics*, vol. 64, no. 2-3, pp. 439–447, Dec. 2001.

[7] J. Schmid and N. Magnenat-Thalmann, "MRI bone segmentation using deformable models and shape priors," *Medical Image Computing and Computer-Assisted Intervention (MICCAI)*, vol. 11, no. Pt 1, pp. 119–126, 2008.

[8] K Akiyama, T Sakai, J Koyanagi, H Yoshikawa, and K Sugamoto, "Evaluation of translation in the normal and dysplastic hip using three-dimensional magnetic resonance imaging and voxel-based registration," *Osteoarthritis and Cartilage*, vol. 19, no. 6, pp. 700–710, June 2011.

[9] Y. Xia, S. S. Chandra, O. Salvado, J. Fripp, R. Schwarz, L. Lauer, C. Engstrom, and S. Crozier, "Automated MR Hip Bone Segmentation," in *Digital Image Computing: Techniques and Applications (DICTA)*, 2011, pp. 25 – 30.

[10] A. Watanabe, C. Boesch, K. Siebenrock, T. Obata, and S. E. Anderson, "T2 mapping of hip articular cartilage in healthy volunteers at 3T: a study of topographic variation," *Journal of Magnetic Resonance Imaging*, vol. 26, no. 1, pp. 165–171, July 2007.

[11] J. Folkesson, E. Dam, O. F. Olsen, P. Pettersen, and C. Christiansen, "Automatic segmentation of the articular cartilage in knee MRI using a hierarchical multi-class classification scheme," in *Medical Image Computing and Computer-Assisted Intervention (MICCAI)*, vol. 3749, pp. 327–334. Springer Berlin Heidelberg, Berlin, Heidelberg, 2005.

[12] P. A. Yushkevich, J. Piven, H. C. Hazlett, R. G. Smith, S. Ho, J. C. Gee, and G. Gerig, "User-guided 3D active contour segmentation of anatomical structures: significantly improved efficiency and reliability," *NeuroImage*, vol. 31, no. 3, pp. 1116–1128, July 2006.

[13] T. F. Cootes, C. J. Taylor, D. H. Cooper, and J. Graham, "Active Shape Models-Their Training and Application," *Computer Vision and Image Understanding*, vol. 61, no. 1, pp. 38–59, 1995.